



Cell diameter doesn't affect lipid productivity of *Chlorococcum littorale*



Iago Teles Dominguez Cabanelas ^{a,b,*}, Carolina Fernandes ^a, Dorinde M.M. Kleinegris ^{b,1}, René H. Wijffels ^{a,c}, Maria J. Barbosa ^{b,1}

^a Wageningen University, Bioprocess Engineering, AlgaePARC, P.O. Box 16, 6700 AA Wageningen, Netherlands

^b Wageningen UR, Food & Biobased Research, AlgaePARC, Bornsesteeg 10, Building 112, 6721NG Bennekom, Netherlands

^c Faculty Biosciences and Aquaculture, University of Nordland, N-8049 Bodø, Norway

ARTICLE INFO

Article history:

Received 30 September 2015

Received in revised form 31 December 2015

Accepted 6 February 2016

Available online 23 February 2016

Keywords:

Microalgae

Chlorococcum littorale

Cell sorting (FACS)

Cell diameter

Biomass productivity

Lipid productivity

ABSTRACT

We hypothesized that cells with different diameter have different division rates, which could affect lipid productivity (lipid content × biomass productivity). In the present work we assessed the influence of cell diameter, as a sorting parameter, on both biomass and lipid productivity of *Chlorococcum littorale*. Prior to sorting, cells were grown in a batch-wise nitrogen run-out including a long nitrogen depleted phase (N−) to stop cell division, thus only having vegetative cells (Pre-sorting). Cell sorting was done at the end of this N− phase using FACS (fluorescence assisted cell sorting) based on forward scatter as a proxy for diameter (size ranges (μm): 5–6 (small), 8–9 (medium), 11–14 (large) and 5–14 (control)). The sorting was done in 2 pools: multiple-cell (100 cells) and single-cell. After sorting, cells were recovered under low-light for 2 weeks, and used to start the Post-sorting experiment (analogous to Pre-sorting). The populations derived from different sorted pools, single-cell and multiple-cell, showed similar size distributions after re-growth. No difference was observed in biomass and lipid productivities among Post-sorting cells and when compared to Pre-sorting cells under nitrogen depletion. We concluded that cellular size had no effect on both biomass and lipid productivity of *C. littorale*.

© 2016 The Authors. Published by Elsevier B.V. This is an open access article under the CC BY license (<http://creativecommons.org/licenses/by/4.0/>).

1. Introduction

Microalgae have shown potential to replace current feedstock for bulk commodities [11,36]. The positive aspects of microalgae bulk production include sustainability and versatility of the production chain when compared to land crops [10]. Nevertheless, reported biomass and lipid productivities need to be improved to make bulk production economically feasible for commodity products, such as plastics or fuels [26,28].

One approach to increase productivity is to develop more productive strains. This can be done by taking advantage of the natural genetic variability of a parental population to screen and sort cells with different features (e.g. high lipid producers) [22,37]. Another possibility is to increase genetic variability by inducing mutations in a parental population and screen and sort for mutants with abnormal improved features [7,13,32,35]. Fluorescence assisted cell sorting (FACS) is a method which allows rapid screening and sorting of cells with desired characteristics. Sorted cells can be regrown, possibly leading to a new improved culture [13,32,35,37]. FACS can sort cells based on multiple

fluorescence and light scattering parameters, which makes it a versatile technology.

Chlorococcum littorale has a high lipid content [29], high photosynthetic efficiency under nitrogen stress [3], and has been used in FACS before [9] and for this reason has been chosen in this study. *C. littorale* is a unicellular microalga whose cell size can range from 5 to 14 μm in the vegetative stage [25]. *C. littorale* can reproduce sexually and asexually by multiple-fission of the mother cell, into 2 to 16 daughter cells (in the shape of spores that can be haploid or diploid, in case of asexual or sexual reproduction, although there is no morphological differences between the two kinds of spores) [25]. The formation of spores is relevant for the sorting, since dividing cells could be mistaken for a large vegetative cell. Up to now the regulation of cell size in microalgae is not completely understood [4,27,33]. Studies with *Chlamydomonas*, a genus with multiple-fission cell division, showed a positive correlation between mother cell's sizes and the number of generated daughters [27]. Other authors have shown that cells might even continue their division without doubling their cell volume. Hence, such cells would produce bigger daughter cells, that would generate more and smaller cells in the next division [4]. Both studies point to a possible influence of cell diameter on the growth patterns of following generations. Up to date, no report has focused on the possible effect of size of vegetative cells on the biomass productivity of bulk cultures. We hypothesized that cells with different diameter have different division rates, which could

* Corresponding author at: Wageningen University, Bioprocess Engineering, AlgaePARC, P.O. Box 16, 6700 AA Wageningen, Netherlands.

E-mail address: iago.dominguezteles@wur.nl (I.T.D. Cabanelas).

¹ www.AlgaePARC.com.

affect biomass productivity. Hence, differences in biomass productivity could consequentially affect lipid productivity (lipid content \times biomass productivity).

In the present work we assessed the influence of cell diameter, as sorting criterion, on both biomass and lipid productivity of vegetative cells of *C. littorale*. *C. littorale* was grown in a batch-wise nitrogen run-out followed by a long nitrogen-depleted phase to stop cell division and to induce lipid accumulation, thus having only vegetative, lipid-rich cells. At the end of the nitrogen-depleted phase (15 days, after cell size was stable) cells were sorted in four groups of different diameters: small ($5\text{--}6 \mu\text{m}$), medium ($8\text{--}9 \mu\text{m}$), large ($11\text{--}14 \mu\text{m}$) and a control ($5\text{--}14 \mu\text{m}$). We compared both biomass and lipid productivities of sorted cells of *C. littorale* with the growth of the parental population. Additionally, we compared the daily differences in cell size distribution, photosystem II quantum yield, autofluorescence and intra-cellular lipid fluorescence.

2. Materials and methods

2.1. Inoculum preparation, cultivation and culture screening with FACS

Inoculum of *C. littorale* (NBRC 102761) was prepared from samples preserved under low light conditions ($16 \mu\text{mol m}^{-2} \text{s}^{-1}$) in borosilicate tubes containing growth medium and agar (12 g l^{-1}). Small samples were transferred from agar to 200 ml sterile borosilicate Erlenmeyer flasks, containing 100 ml of sterile growth medium. *C. littorale* was grown in salt water-like medium with the following composition (g l^{-1}): NaCl 24.55, MgSO₄·7H₂O 6.60, MgCl₂·6H₂O 5.60, CaCl₂·2H₂O 1.50, NaNO₃ 1.70, HEPES 11.92, NaHCO₃ 0.84, EDTA-Fe(III) 4.28, K₂HPO₄ 0.13, KH₂PO₄ 0.04. The medium also contained the following trace elements (mg l^{-1}): Na₂EDTA·2H₂O 0.19, ZnSO₄·7H₂O 0.022, CoCl·6H₂O 0.01, MnCl₂·2H₂O 0.148, Na₂MoO₄·2H₂O 0.06, CuSO₄·5H₂O 0.01.

The sequence of experiments performed in this work is represented in Fig. 1. After inoculum preparation we set-up a preliminary test to determine the boundaries for the sorting gates based on cell size using fluorescence assisted cell sorting (FACS). The preliminary test was performed before but analogous to the experiment explained in the next section.

2.2. Experimental set-up

The experimental set-up was the same for both Pre-sorting and Post-sorting experiments (Fig. 1). Experiments were inoculated with an initial OD₇₅₀ value of 0.5 ($\sim 0.7 \text{ g DW l}^{-1}$). The algae were cultivated in 200 ml borosilicate Erlenmeyer flasks (100 ml medium per flask) and kept in an Infors Multitron Pro orbital shaker incubator. Growth conditions were: $25 \pm 0.2^\circ\text{C}$, 120 rpm, 60% humidity, 2% CO₂ enrichment on air, and $120 \pm 2 \mu\text{mol m}^{-2} \text{s}^{-1}$ continuous light (24 h).

Both experiments had 2 phases: a growth phase (N+) and a nitrogen depleted (N-) phase. During the growth phase nitrogen (N-NO₃) was allowed to run-out progressively (at day 5 NO₃ was completely consumed by the cells). After reaching stationary phase, the cultures were diluted 5× to a biomass concentration of $1.4 \pm 0.1 \text{ DW g l}^{-1}$, in sterile medium without NO₃⁻, to allow further light penetration in the culture and enhance lipid production. After dilution, cells were monitored until maximum size was achieved, and was constant for 3 days (after 15 days from start experiment). All daily measurements were done at the same time every day and are described in the following section.

Multiple-cell sorting (3×100 cells) was done based on cell size in four groups, at the end of the stationary phase (Fig. 3). After sorting, cells were re-suspended in 50 ml sterile falcon tubes containing fresh and sterile nitrogen-replete medium into. Cells grew for 2 weeks in the tubes under low light conditions ($16 \mu\text{mol m}^{-2} \text{s}^{-1}$). After this, cells were transferred to sterile borosilicate Erlenmeyer's, where Post-sorting experiments were conducted under similar conditions as the Pre-sorting experiments and with the same daily measurements.

Additionally single-cells were sorted from the same parental population on the same day (Fig. 1). Fifteen replicates per group of single-sorted cells were taken to increase sample size and to assure reproducibility of Post-sorting results. Single cell sorting was done analogous to and immediately after the multiple-cell sorting. After 18 days of growth under low-light conditions ($16 \mu\text{mol m}^{-2} \text{s}^{-1}$) the sorted cells were centrifuged at $1224 \times g$ for 10 min, washed with sterile medium and readily analyzed for size and autofluorescence using the FlowCAM® fluid imaging system (settings are presented in the next section).

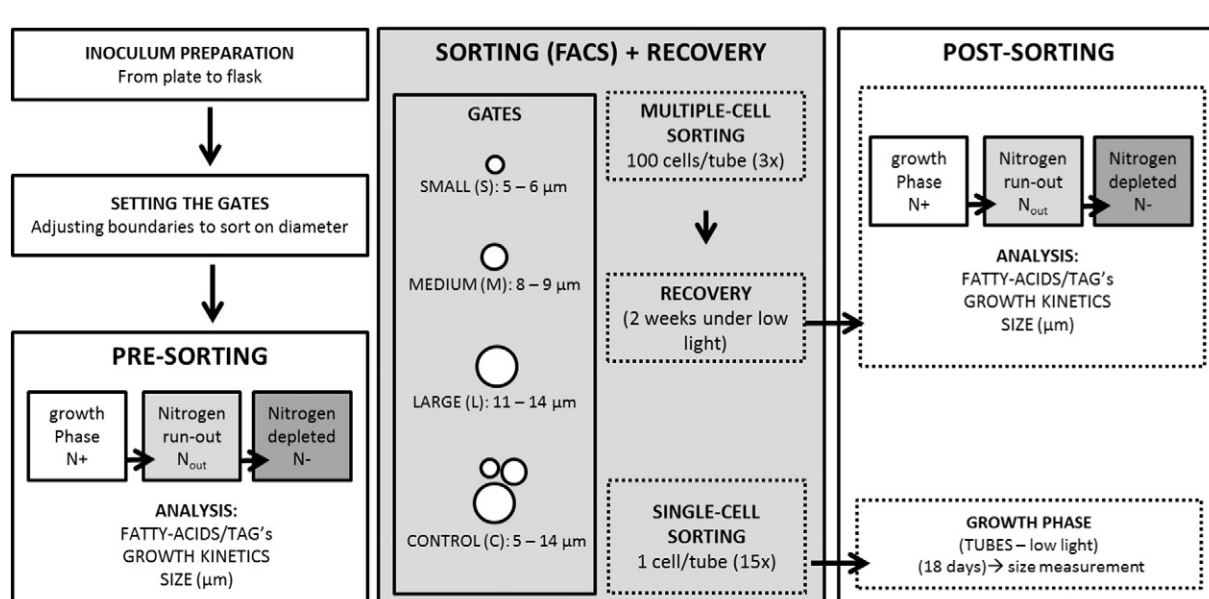


Fig. 1. Experimental flow diagram followed in this work. Inoculum preparation: fresh cultures were prepared from agar plate's cultures and kept under controlled conditions. Setting the gates: a preliminary test was done to set the boundaries of the gates used for the actual sorting. Pre-sorting: Batch nitrogen run-out cultivations were done in flasks including a growth phase (N+, in white), a nitrogen run-out (N_{out}, in light gray) and a nitrogen depleted phase (N-, in dark gray). The same colors were used in Figs. 4 and 7. Sorting: after cell size was stabilized during nitrogen depletion (3 days with the same size distribution) the multiple-cell sorting was done with 4 different gates based on size (3×100 cells/replicate). Post-sorting: experiments analogous to Pre-sorting to compare biomass and lipid productivities; the single-cell sorted cells were readily analyzed after 18 days of re-grow. Acronyms: FACS (fluorescence assisted cell sorting) and TAG's (triacylglycerides).

2.3. Daily measurements

All daily measurements were done at the same time every day. Optical densities were measured on a daily basis using a spectrophotometer (HACH, DR5000) on two different wavelengths: 680 and 750 nm. Samples were diluted within the range of the detection limit (0.1–1 units of OD). OD₇₅₀ was used as a proxy for biomass concentration and OD₆₈₀ was relative to the chlorophyll fluorescence [16].

Quantum yield of photosystem II (PSII) – ratio between the number of photons emitted and the number of photons absorbed by the cells – was measured daily with a fluorometer (AquaPen-C AP-C 100, Photon System Instruments, Czech Republic). The measurements were done with cultures at OD₇₅₀ values between 0.2–0.4 after a dark period of 10 min at room temperature. The quantum yield was used to infer the photochemical efficiency of the cells. The F_v/F_m ratio gives the maximum quantum yield of PSII (Eq. (1), [3]), where F₀ is the minimal level of fluorescence (after dark-acclimation) and F_m is the maximum fluorescence after exposing the cells to a pulse of actinic light.

$$(F_v/F_m) = \frac{F_m - F_0}{F_m} \quad (1)$$

FlowCAM® analyses were performed daily to follow-up the cell's diameter, autofluorescence (chlorophyll fluorescence) and lipid-dependent fluorescence (BODIPY_{505/515} fluorescence). For FlowCAM® analyses samples were first diluted 100 to 1000 times and then stained for neutral lipids to achieve a final concentration of 0.4 µg/ml of BODIPY_{505/515} and 0.35% of ethanol, following the protocol of [9]. After 5 min the samples were run in the FlowCAM® (Fluid Imaging Technologies, Yarmouth, Maine) using the following settings: 20× optical magnification and Trigger-mode-on with channels 1 and 2, autofluorescence (650 nm long pass filter) and BODIPY_{505/515} (525/30 filter), respectively. The trigger mode activates the system to take a camera image when a particle produces a fluorescence signal. Diameter (µm), autofluorescence (Ch1) and BODIPY_{505/515} fluorescence (Ch2) of each sample were taken for further analyses.

Daily samples were taken for measurement of nitrogen content (N–NO₃ mg l⁻¹) in the medium. 1 ml of culture was centrifuged at 13,000 × g and the supernatant was used for analysis. Nitrogen content was measured daily with the Sulphanilamide N-1-naphthyl method (APHA 4500-NO3-F) using the SEAL AQ2 automatic analyzer.

2.4. Cell sorting using FACS

At the end of the nitrogen-depleted phase of the Pre-sorting experiment, a sample was collected and diluted to an OD₇₅₀ of approximately 0.3, to keep cell concentration in the flow cytometer at 200 cells/min. The sorting was carried out with a FACScalibur® flow cytometer (BD Biosciences, San Jose, California). FACScalibur® is equipped with an argon ion laser with excitation at 488 nm and in our work the emission at 670LP (FL3 channel) was used, relative to the cells autofluorescence (Chlorophyll-a emission). FL3 channel was read in logarithmic scale and the sensitivity was set at 300 mV while FSC channel was read on linear scale. Cells were collected in sterile 50 ml falcon tubes and sterile PBS was used as sheath fluid (phosphate saline buffer; composition: NaCl 137 mM, KCl 2.7 mM, Na₂HPO₄ 10.0 mM, KH₂PO₄ 1.8 mM).

The sorting was done in two steps: multiple-cell sorting and single-cell sorting. For multiple-cell sorting 100 cells were collected per tube to produce inoculum for the Post-sorting experiments (in triplicate). Subsequently, single-cell sorting was carried-out using the same sample and same machine settings as the multiple-cell sorting (with 15 replicates for each size). After sorting, cells were centrifuged at 1224 × g for 5 min and re-suspended in sterile growth medium (both multiple and single-cell sorting). The tubes with sorted cells were placed under constant light at 16 µmol m⁻² s⁻¹, allowing cells to recover for 2 weeks. After the recovery time, triplicates containing 100 cells each

were transferred to Erlenmeyer flasks to produce inocula for the Post-sorting experiments. The cultures originating from the single-cell sorting experiments were readily analyzed with the FlowCAM® after 18 days of growth in the tubes.

2.5. Fatty acid and TAG analysis

Biomass samples were collected at the end of both nitrogen replete (N+) and nitrogen depleted (N-) phases of Pre- and Post-sorting experiments. Biomass was centrifuged twice and washed with MilliQ water (3134 × g for 10 min at 4 °C) and followed by freezing at –20 °C and freeze-drying for 24 h.

Fatty acid and triacylglycerol's (TAGs) extraction and quantification were performed as described by Breuer et al. [8], using GC/MS column chromatography of the chloroform fraction of lipids.

2.6. Data analysis

Data from FlowCAM and cytometer were exported to Microsoft Excel to be edited and analyzed. For statistical analysis, one-way analysis of variance (ANOVA) was used to access the significance of differences between and among sorted groups (SigmaPlot, v. 12.5). The premises of ANOVA, i.e. the homogeneity of variances and the normality of the data, were also measured with SigmaPlot. A p-value lower than 0.05 was considered significant.

2.6.1. Calculations

The biomass dry weight was used to calculate the growth rate of *C. littorale*, as given in [Eq. (2)],

$$\mu = \frac{\ln (DW_{t_{final}} - DW_{t_0})}{t_{final} - t_0} \quad (2)$$

where, DW stands for the dry weight of biomass (g l⁻¹), from the first (t₀) and the last time point (t_{final}) considered. For the growth rate under nitrogen replete conditions (N+) the 5th day of cultivation (d = 5) and the day of inoculation (d = 0) were used as final and initial values, respectively.

The increase in BODIPY cellular fluorescence was used to calculate the BODIPY accumulation rate (BP_r), relating to the increase of cellular neutral lipids in time. The BP_r was estimated with a similar approach as used for Eq. (2), only that the values of DW were replaced with the values of BP fluorescence (relative fluorescence units, RFU). The period of time used for calculation was the period between the start (d = 5) and the end (d = 10) of the nitrogen run-out (being d = 0 the inoculation day). This period was chosen because it shows the first increase in intracellular lipid content; hence it is an estimate of the first metabolic response of the intracellular lipid accumulation.

The decrease in photosystem II quantum yield (QY_r) was calculated using an identical approach to the one used in Eq. (2), but replacing DW values by QY measurements. Two QY_r were calculated: at the end of the nitrogen run-out (between d = 5 and d = 10), and at the end of the nitrogen depleted phase (between d = 10 and d = 25).

The volumetric biomass productivity (P_x, g l⁻¹ d⁻¹) is given by [Eq. (3)],

$$P_x = \frac{DW_{t_{final}} - DW_{t_0}}{t_{final} - t_0} \quad (3)$$

where, two time intervals of the dry weight (DW, in g per liter) were used: between the end (d = 10) and the beginning (d = 5) of the nitrogen run-out (N_{out}) and at the end (d = 25) and the beginning (d = 10) of the nitrogen depleted phase (N-).

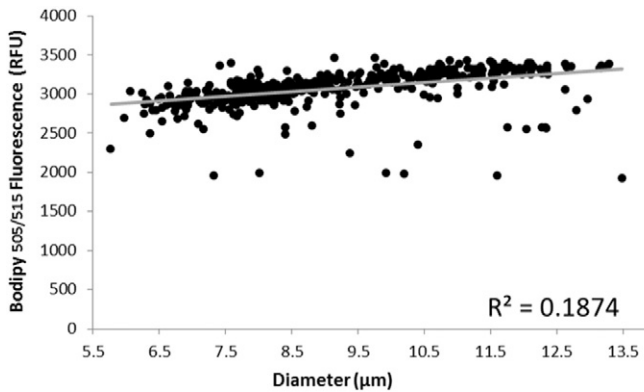


Fig. 2. Nitrogen stressed cells show no correlation between diameter and intracellular lipid-fluorescence: Scatter plot between BODIPY dependent fluorescence (y-axis) and cellular diameter (x-axis) ($n = 500$ cells). Data derived from the preliminary test, with cells exposed to 15 days of nitrogen depletion. R^2 represents the coefficient of determination, evidencing the lack of correlation between lipid-dependent fluorescence and cellular diameter.

The final TAG volumetric productivity (P_{TAG} , $\text{mg l}^{-1} \text{d}^{-1}$) was estimated using [Eq. (4)],

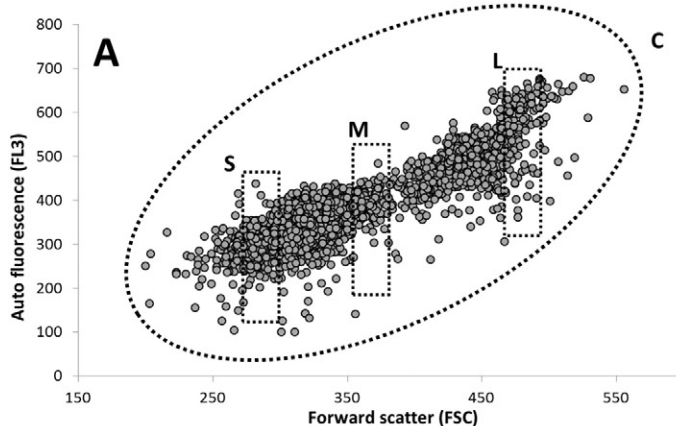
$$P_{TAG} = (P_X \times \text{TAG}) \times 1000 \quad (4)$$

where P_X is the biomass volumetric productivity calculated above and the TAG (triacylglycerides) content in the biomass (g g^{-1}). The P_{TAG} was calculated using the P_X and the TAG content from both N_{out} and $N -$ phases.

3. Results and discussion

3.1. Gate set-up to sort cells on size

A preliminary test was done to check 2 assumptions: 1] that the intracellular lipid content is not correlated with the cell diameter and 2] that FACS could be used to sort cells based on cell size. The first assumption is relevant not to include the lipid content as a sorting criteria. As stated in the introduction, we hypothesized that cells with different diameters can have different division rates and we want to evaluate the effect of such differences on lipid productivity. We found no correlation between cell diameter and intracellular lipid-fluorescence, as it can be seen from the R^2 value in Fig. 2. The preliminary test was done using the same experimental set-up as it was used for the actual experiments (Fig. 1 and Section 2.2 of methods).



Once the first assumption was checked we used the same sample to do a preliminary sorting test to check the second assumption: can FACS be used to sort cells based on diameter? Cell diameter cannot be directly measured in FACS. However, measurements of the forward light scattering (FSC) of every cell can be used as a proxy for cell size [2,37]. Although calibration beads are available to convert FSC into diameter [23], we decided not to use calibration beads due to intrinsic differences in e.g. surface smoothness between the calibration beads and microalgae cells. Furthermore, we worked with size intervals that differed from each other in only 2 μm . Hence we decided not to use calibration beads to convert FSC to cell size, instead we decided to use FSC as a proxy for cell size and to perform a test to confirm the results of the set gates boundaries by measuring the cell size of sorted cells immediately after the sorting (using FlowCAM fluid imaging).

A histogram of FSC was firstly established to show the distribution of size within the population and to identify the different size groups (Fig. 3B). The information from the histogram (Fig. 3B) was crosschecked with simultaneous plotting of autofluorescence (AF) versus FSC (Fig. 3A) as a positive control for algae cells (to avoid gating non-fluorescent particles). Autofluorescence was used as a proxy for cellular chlorophyll content to confirm the identity of the particles as microalgae cells. We kept the ratio AF/FSC the same for all gates to avoid AF as a second sorting criteria (Small: 1.2, Medium: 1.1, and Large: 1.1). The gates used for sorting were established on the dot-plot shown on Fig. 3A. This approach was important to avoid the inclusion of cell debris, especially for the group containing small cells.

Once the gates were established, as shown in Fig. 3A, the cells were sorted (100 cells per group, in triplicate) and subsequently analyzed for size. The cell size was assessed with the FlowCam imaging, which provides direct measurement of cell diameter (μm) and autofluorescence, supplementing the analysis from FACS. The results from the preliminary test (Fig. 3) confirmed the suitable gate boundaries to sort cells based on size: small (5–6 μm), medium (8–9 μm), large (11–14 μm) and a control including all previous sizes (5–14 μm). Detailed pictures of the cells from all different groups can be found in the supplementary materials (SM1).

3.2. Growth of *C. littorale* before cell sorting

C. littorale was cultivated phototrophically, batch wise in nitrogen replete medium (Pre-sorting experiment). At day 5 the concentration of nitrogen in the medium was zero (Fig. 4A, light gray area marks the 5th day). We kept the cultivation for 5 additional days after nitrogen run-out, until biomass concentration reached its maximum, meaning that the cells had consumed their internal nitrogen pools while finishing to divide (which can also be noticed on the size evolution, Fig. 4C). At

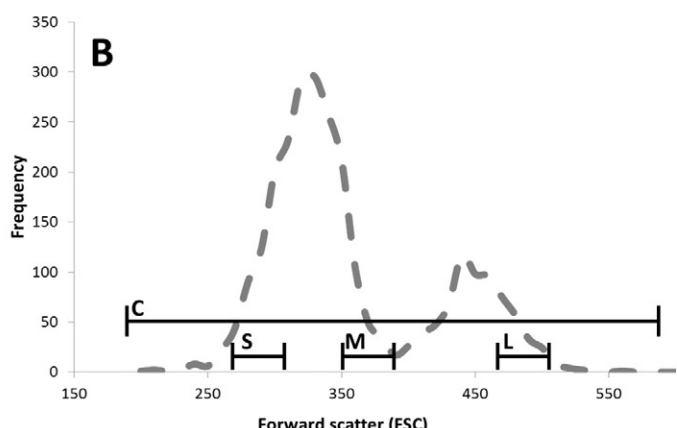


Fig. 3. Preliminary test done to set the boundaries to sort cells based on size. A: Dot-plot of nitrogen depleted cells of *Chlorococcum littorale* using Auto fluorescence (FL3) vs forward scatter (FSC), both parameters are in relative fluorescence units (RFU). B: Histogram of frequency of the FSC of nitrogen depleted cells of *Chlorococcum littorale*. The gates are depicted as rectangles and an ellipse (A) and range-lines (B) and stand for small (S), medium (M) and Large (L) and control (C).

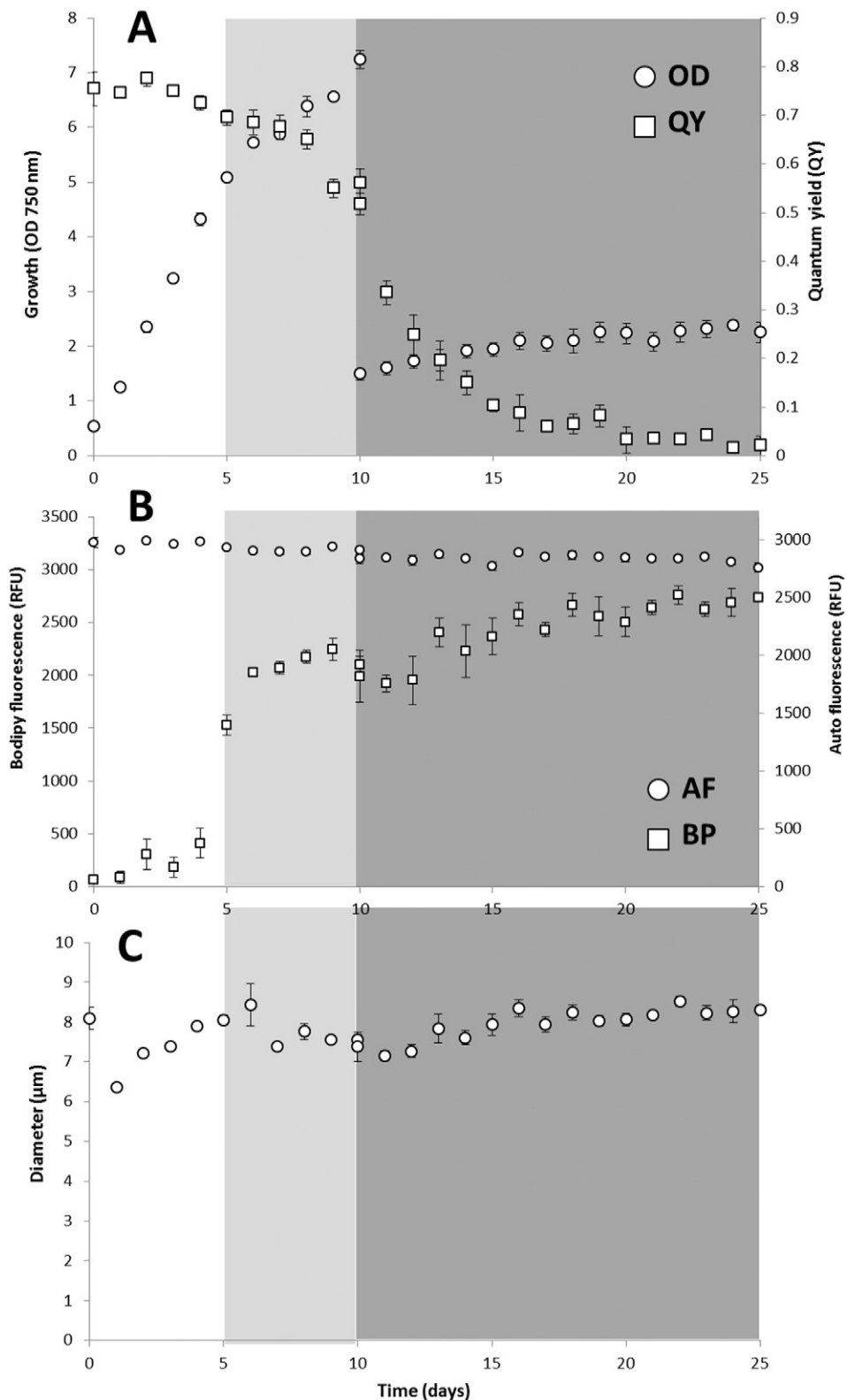


Fig. 4. Evolution of *C. littorale* growth parameters before cell sorting. The white area of the chart indicates the growth phase ($N+$), the light gray area marks the point in which N runs out (N_{out}), and the dark gray area indicates the phase in which the culture is diluted in nitrogen depleted medium ($N-$). For every plot the standard deviation is present, ($n = 3$). A: Evolution of biomass production of *C. littorale* (circles, primary y-axis) and evolution of the quantum yield of photosystem II over time (QY, squares, secondary y-axis). B: Evolution of autofluorescence (circles, primary y-axis) and BODIPY-fluorescence (squares, secondary y-axis) of *C. littorale* cells over time. The averages of two measurements of fluorescence were plotted (500 cells were assessed per measurement). The measurements are represented as relative fluorescence units (RFU). C: Evolution of average (per cell) diameter of *C. littorale* cells over time.

this point, the cultures were diluted in nitrogen depleted medium to increase the light intensity inside the culture necessary to further stimulate lipid accumulation in microalgae [18,21,30,34] (Fig. 4A), and a consequent increase in size (Fig. 4C).

Table 1 presents the growth rate, biomass and TAG volumetric productivities and fatty-acid and TAG content (%DW biomass). The growth rates and productivities calculated in the present work were used to compare the Pre-sorting with the Post-sorting populations.

In the growth phase we observe that the quantum yield (QY) of photosystem II remained above 0.5, supporting the hypothesis that the cells were not under photochemical stress (Fig. 4A). The QY is an indicator of stress at values below 0.4 [19,38]. We can detect a drop in the QY after the nitrogen run-out (light gray area, Fig. 4A) and a further drop to half of the initial value during the nitrogen depleted phase (dark gray area, Fig. 4A). Low values of QY are an indirect indication of lipid formation, because under nitrogen stress no biomass can be produced and the photochemical energy is used to produce storage lipids [1]. The experiment was kept until values of QY close to 0 were achieved (Fig. 4A).

Both autofluorescence and lipid-related fluorescence (BODIPY) were monitored during the experiment. The autofluorescence was stable throughout the experiment, showing only a reduction of 6.8% in autofluorescence from the beginning to the end of the experiment (Fig. 4B). The autofluorescence is related to the fluorescence of both photosystems in the chloroplast [14], hence it can be used as a proxy for the chlorophyll content per cell. We can infer that almost no chlorophyll degradation took place, since only a small fraction of autofluorescence was reduced.

Fluorescence of the BODIPY dye was used as a proxy for cellular lipid content [2,9,15,24]. BODIPY_{505/515} is a dye used to stain non-polar lipid bodies in microalgae cells [9,12,24]. The average BODIPY_{505/515} fluorescence per cell is presented in Fig. 4B, where it is possible to see an accumulation of neutral lipids from the moment of nitrogen run-out onward (Day 5). The increase in cellular lipid content is a survival mechanism in most microalgae, which directs the energy converted from photosynthesis to the synthesis of storage lipids in the absence of substrate (nitrogen) to grow [1,17,20].

3.3. Single-cell and multiple-cell sorted populations exhibited similar size distribution

Sorting based on cell size took place at the end of the nitrogen-depleted phase ($d = 25$), after vegetative cells had reached their maximum size (As showed in 4C). Size measurements were plotted in a histogram after the regrowth phase (Fig. 5). The overlap of the curves indicates that, after sorting, cells showed the same behavior as before the sorting. We also measured the distribution of cell diameter in the population originated from sorted single-cells to compare the 4 sorted populations among each other. The comparison of the average cell

diameter among the sorted cells showed no statistical difference (Fig. 6, $p > 0.05$, one-way ANOVA).

These results were the first evidence that cell size might be an intrinsically regulated phenotypical distribution of *C. littorale*. Cell cycle studies with *Chlamydomonas*, a microalgae strain with multiple-fission division as *C. littorale*, showed that there is a positive correlation between mother cell's sizes and the number of generated daughters [27]. Other authors, however, have shown that cells might divide without doubling their cell volume. Hence, such cells would produce bigger daughter cells, that would generate more and smaller cells in the next division, which is an evolutionary advantage for natural unstable conditions [4].

3.4. Cell size showed no effect on the growth dynamics of *C. littorale* after sorting

All sorted populations were grown batch wise in similarity to the Pre-sorting experiment (Fig. 4) in order to be able to compare the Pre-with the Post-sorting culture on biomass and lipid productivity. All populations, including the parental population, showed similar growth (Fig. 7 and Table 1).

All four groups showed similar biomass productivities during the nitrogen run-out phase, ranging from 0.32 to $0.35 \text{ g l}^{-1} \text{ d}^{-1}$ ($P_x N_{out}$, Table 1). The lack of statistical difference among the groups confirms the previous results from the size distribution of single cell and multiple-cell sorting's (Figs. 5 and 6). The Post-sorting populations showed, however, a higher value of P_x at N_{out} when compared with the Pre-sorting population ($P_x N_{out}$, Table 1, $p < 0.05$). The higher P_x values from Post-sorting could be a result of the low light acclimation that the cells experienced during recovery (Fig. 1), before being again cultivated, which is known to increase photosynthetic efficiency, hence, the biomass production [5]. Another observation that could corroborate this effect is the evolution of the photosystem II quantum yield (QY) (Fig. 7). The QY values dropped at a faster rate in the Pre-sorting experiment when compared with the Post-sorting experiment (Figs. 4 and 7). The evolution of the QY, however, showed no difference when Post-sorting populations were compared among each other (Fig. 7). This effect can also be seen with the similar QY decrease rates (QY_{rate}) between experiments at the end of both N+ and N- phases (from 0.3 to 0.4, Table 1).

Despite an apparent physiological change possibly due to photoacclimation during nitrogen replete conditions, no difference was observed in the P_x among the sorted groups and in comparison with the Pre-sorting population at nitrogen depleted conditions ($P_x N^-$, Table 1). These results are evidence that cell size of vegetative cells has no effect, as sorting criteria, on biomass productivity.

The evolution of BP fluorescence over time (Fig. 7B) is related to the values of lipid productivity (Table 1). All sorted populations showed similar trends among each other (Fig. 7) and when compared to the Pre-

Table 1
Growth parameters of *C. littorale* Pre- and Post-sorting. Growth rate (μ) is presented only for the growth phase (N+) (white area of Figs. 3 and 6). Decrease rates of photosystem II (QY_r) are presented for the nitrogen run out period (N_{out}) and N-depleted phase (N-) (As depicted in Figs. 3 and 6: N_{out} refers to the light gray area while N- refers to the dark gray area). BODIPY accumulation rate (BP_r) is related to the lipid accumulation after nitrogen run-out (N_{out}). The volumetric productivities of biomass (P_x) and TAG's (P_{TAG}) and also the total fatty acids and TAGs content (%DW) are presented for both growth phase (N+) and nitrogen depleted phase (N-). Superscript letters (a, b and c) mean statistical significance (ANOVA, $p < 0.05$). Statistical analysis was carried out to detect differences between the Pre- and Post-sorting experiments.

Parameter	Phase	Pre-sorting	Post-sorting			
			Control	Small	Medium	Large
$\mu (\text{d}^{-1})$	N^+	0.19 ± 0.00	0.19 ± 0.00	0.17 ± 0.00	0.17 ± 0.00	0.18 ± 0.00
$QY_r (\text{d}^{-1})$	N_{out}	-0.34 ± 0.05	-0.40 ± 0.04	-0.46 ± 0.09	-0.49 ± 0.10	-0.44 ± 0.05
	N^-	-0.04 ± 0.00	-0.04 ± 0.01	-0.05 ± 0.00	-0.05 ± 0.00	-0.05 ± 0.00
$BP_r (\text{d}^{-1})$	N_{out}	1.27 ± 0.05	1.39 ± 0.05	1.29 ± 0.08	1.46 ± 0.05	1.33 ± 0.02
$P_x (\text{g l}^{-1} \text{ d}^{-1})$	N_{out}	0.29 ± 0.02^a	0.32 ± 0.06^b	0.32 ± 0.01^b	0.35 ± 0.02^b	0.31 ± 0.02^b
	N^-	0.07 ± 0.00^a	0.07 ± 0.00^a	0.09 ± 0.00^a	0.08 ± 0.00^a	0.07 ± 0.05^a
$P_{TAG} (\text{mg l}^{-1} \text{ d}^{-1})$	N_{out}	38.25 ± 2.15^a	23.25 ± 1.51^b	22.62 ± 1.80^b	23.87 ± 1.01^b	18.17 ± 1.30^c
	N^-	14.50 ± 0.15^a	12.35 ± 0.20^a	14.82 ± 0.70^a	13.65 ± 0.12^a	13.10 ± 0.11^a
Total TAGs (%DW)	N_{out}	13.19 ± 0.01^a	7.36 ± 0.73^b	7.07 ± 0.35^b	7.46 ± 0.17^b	5.68 ± 0.25^c
	N^-	33.77 ± 0.15^a	25.00 ± 0.07^b	25.6 ± 0.06^b	24.3 ± 0.00^b	24.4 ± 0.02^b

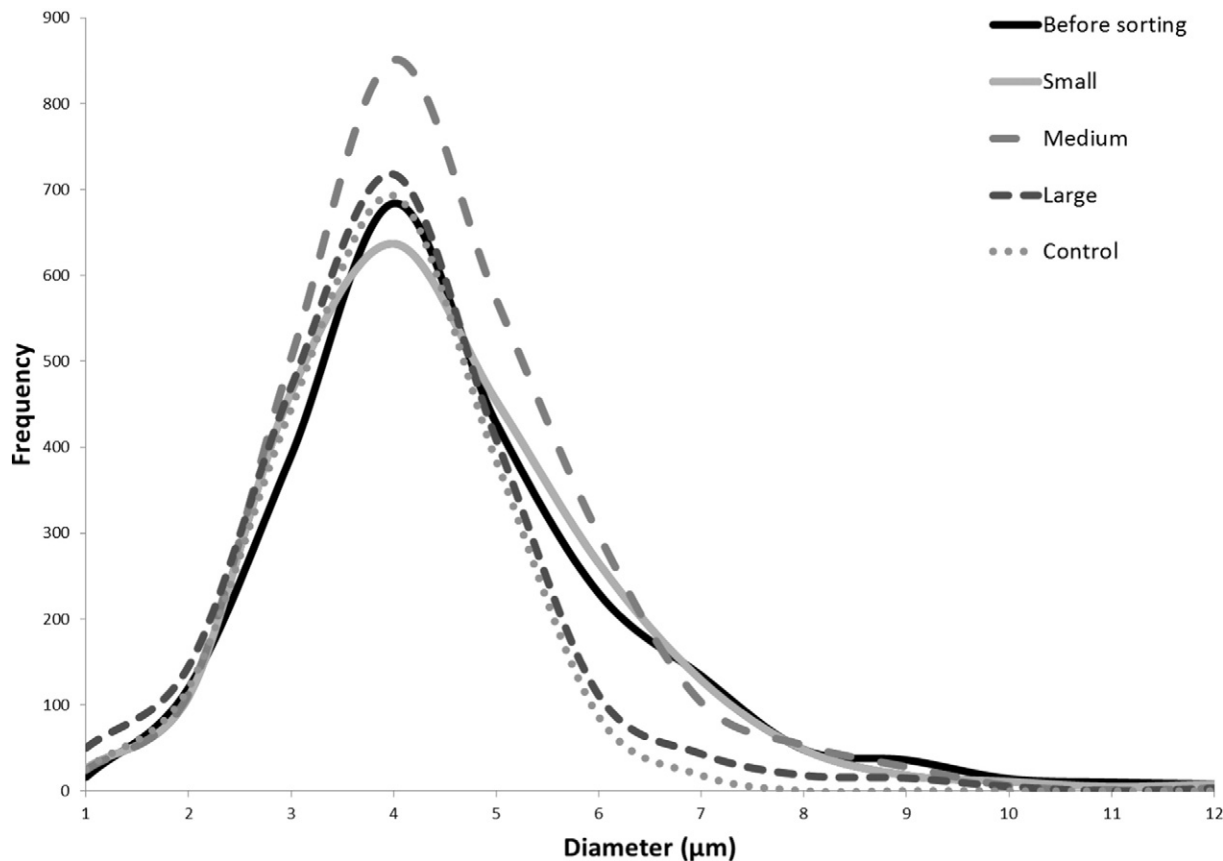


Fig. 5. Cell size distributions of the different sorted populations overlap with the distribution of the parental population. To assess early differences in cell size distribution we measured cell size from all sorted samples after re-growth (after two weeks recovery, as shown in Fig. 1). A sample from the growing inoculum (early exponential phase) from the Pre-sorting experiment was also taken for comparison.

sorting experiment (Fig. 4B) in the evolution of lipid/cell accumulation. However, all sorted populations reached lower values of BP fluorescence at the end of the N_{out} phase when compared with the Pre-sorting experiments (Figs. 4 and 7). Such lower values of BP fluorescence match the results of lipid content in biomass: both TAG/total fatty-acids content and TAG productivity (P_{TAG}) were similar among Post-sorting populations at the end of the N_{out} , but statistically different when compared to the Pre-sorting experiment (Table 1, ANOVA $p < 0.05$). An exception was for both TAG/total fatty-acids content and TAG productivity (P_{TAG}) of large cells (Table 1), which showed values statistically lower than the other Post-sorted populations and the parental population. However, such differences were not found in the $N-$ phase, indicating that the delay in lipid accumulation was temporary during the N_{out} . These differences may be an effect of the low-light acclimation period the sorted cells went through for 2 weeks before growing under the same conditions as the Pre-sorting experiment (as shown in Fig. 1). The photo-acclimation effect is corroborated by the above-mentioned slower decrease in the QY values (Fig. 7A and Table 1). Due to photo-acclimation cells produced more biomass in comparison to the Pre-sorting experiment, which explains the different TAG fluorescence per cell (Fig. 7B) and the lower TAG content/productivity in biomass (Table 1) in the Post sorting experiment.

These results point to a temporary change in the physiological response of sorted cells, seen in the lower values of BP at the beginning of the nitrogen run-out in comparison with the Pre-sorting experiment (Figs. 4 and 7). However, the accumulation rate of BP fluorescence ($BP_r \text{ d}^{-1}$) shows that the biological mechanism still responded at the same rates. Likewise, the P_{TAG} at the end of the nitrogen depletion phase ($N-$) showed no differences among the Post-sorting populations and no difference when compared with the Pre-sorting population (Table 1). We conclude that sorting vegetative cells of *C. littorale*

according to cellular diameter does not result in differences in biomass and lipid productivity.

4. Final remarks

We established the gates for cell sorting based on size using the FSC as a proxy for diameter in combination with autofluorescence. A Pre-

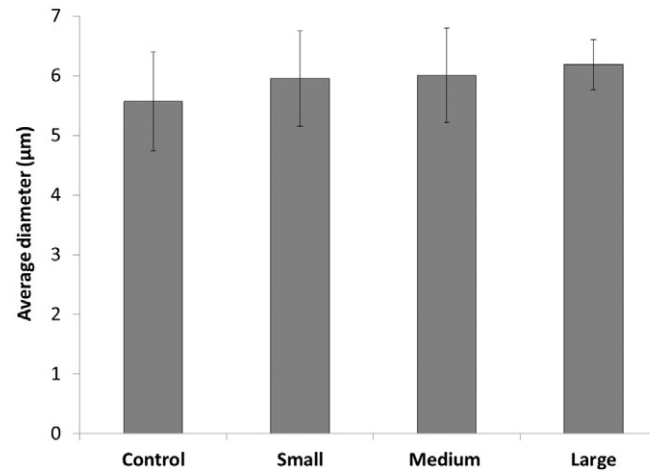


Fig. 6. Single-cell sorted populations showed similar average diameters after re-growth. Gray columns represent the average cell diameter ($n = 500$, per replicate) of each sorted population (originated from a single-cell) after re-growth for 18 days in nitrogen-replete medium and constant light ($16 \mu\text{mol m}^{-2} \text{s}^{-1}$). Error bars represent the standard deviations between replicates. Statistical analysis showed no significant differences ($p > 0.05$, one-way ANOVA).

sorting experiment was performed including a growth phase ($N+$), a nitrogen run-out (N_{out}) and a long nitrogen depleted phase ($N-$). The $N-$ phase assured that cells stopped dividing, thus resulting only in

vegetative cells, and assured that cells only increased their size due to lipid accumulation. Vegetative cells of *C. littorale* were sorted at the end of the Pre-sorting experiment based on cell size. Both single-cell

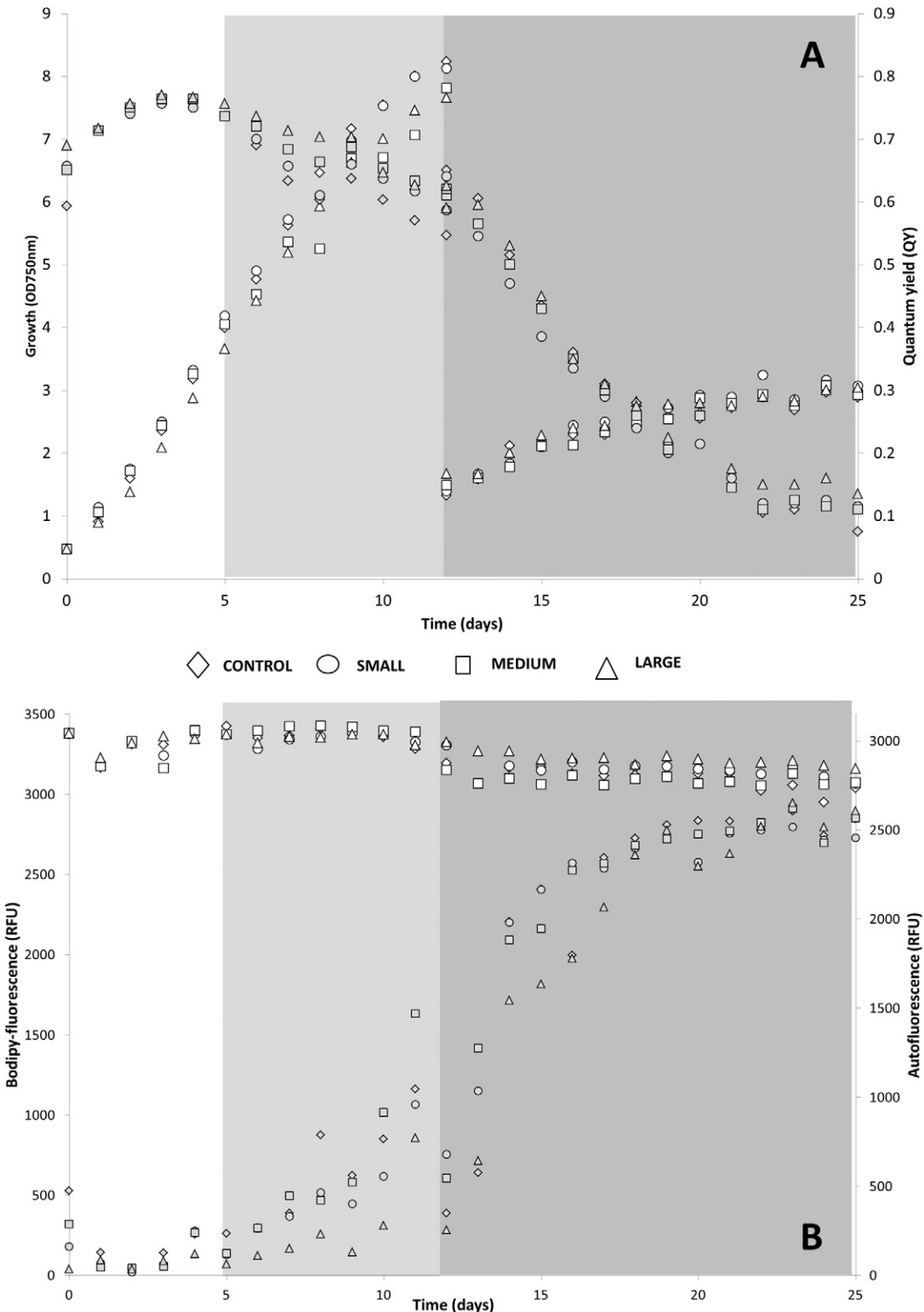


Fig. 7. Different sorted populations exhibited similar growth dynamics among each other. The white area of the chart indicates the growth phase, the light gray marks the start of the nitrogen run-out, and the dark gray area of the chart indicates the phase in which the cultures were diluted in nitrogen-depleted medium. All sorted populations are represented in the graphs: small (○), medium (□), large (△) and control (◊). A: The evolution of biomass production of *C. littorale* (OD₇₅₀) (primary y-axis) and the evolution of the quantum yield (QY) of photosystem II (secondary y-axis) over time. B: The fluorescence of BODIPY (BP) (primary y-axis) shows a sigmoid curve, while the autofluorescence (AF) (secondary y-axis) shows a smooth curve. Both fluorescence signals were measured with the FlowCAM and are given in relative fluorescence units (RFU); values are the average fluorescence per cell of an analyzed population of 500 cells).

and multiple-cell sorted populations showed similar size distributions after re-growth. The growth rates and productivities (biomass and lipid) were calculated to compare Pre- and Post-sorting populations. No difference among Post-sorting populations was detected, however, Post-sorting cells showed a higher value of biomass productivity (P_x) when compared with Pre-sorting cells. This result could be due to the low light acclimation that the cells experienced during recovery after sorting. Nevertheless, no difference was observed in the TAG's productivity (P_{TAG}) among Post-sorting cells and when compared to Pre-sorting cells at the nitrogen depletion phase. We conclude that cellular size of vegetative cells has no effect on both biomass and lipid productivities of *C. littorale*.

Acknowledgments

The authors would like to thank the financial support to AlgaePARC Research Program provided by: Ministry of Economic Affairs, Agriculture and Innovation (the Netherlands), Province of Gelderland (the Netherlands), and the companies: BASF, BioOils, Drie Wilgen Development, DSM, Exxon Mobil, GEA Westfalia Separator, Heliae, Neste Oil, Nijhuis, Paques, Cellulac, Proviron, Roquette, SABIC, Simris Alg, Staatsolie Suriname, Synthetic Genomics, TOTAL and Unilever (TRCDKI/2010/0956). Also, the National Council of Science and Technology (Brazil) is acknowledged for the grant 236614/2012-6.

Appendix A. Supplementary data

Supplementary data to this article can be found online at <http://dx.doi.org/10.1016/j.algal.2016.02.002>.

References

- [1] C. Adams, V. Godfrey, B. Wahlen, L. Seefeldt, B. Bugbee, Understanding precision nitrogen stress to optimize the growth and lipid content tradeoff in oleaginous green microalgae, *Bioresour. Technol.* 131 (2013) 188–194, <http://dx.doi.org/10.1016/j.biotech.2012.12.143>.
- [2] V. Benito, F. Goñi-de-Cerio, P. Brettes, BODIPY vital staining as a tool for flow cytometric monitoring of intracellular lipid accumulation in *Nannochloropsis gaditana*, *J. Appl. Phycol.* (2014) 233–241, <http://dx.doi.org/10.1007/s10811-014-0310-x>.
- [3] G. Benvenuti, R. Bosma, M. Cuartero, M. Janssen, M. Barbosa, R. Wijffels, Selecting microalgae with high lipid productivity and photosynthetic activity under nitrogen starvation, *J. Appl. Phycol.* (2014) 1–7, <http://dx.doi.org/10.1007/s10811-014-0470-8>.
- [4] K. Bišová, V. Zachleder, Cell-cycle regulation in green algae dividing by multiple fission, *J. Exp. Bot.* 65 (2014) 2585–2602, <http://dx.doi.org/10.1093/jxb/ert466>.
- [5] G. Bonente, S. Pippa, S. Castellano, R. Bassi, M. Ballottari, Acclimation of *Chlamydomonas reinhardtii* to different growth irradiances, *J. Biol. Chem.* 287 (2012) 5833–5847, <http://dx.doi.org/10.1074/jbc.M111.304279>.
- [6] G. Breuer, L. de Jaeger, V.P.G. Artus, D.E. Martens, J. Springer, R.B. Draisma, G. Eggink, R.H. Wijffels, P.P. Lamers, Superior triacylglycerol (TAG) accumulation in starchless mutants of *Scenedesmus obliquus*: (II) evaluation of TAG yield and productivity in controlled photobioreactors, *Biotechnol. Biofuels* 7 (2014) 70, <http://dx.doi.org/10.1186/1754-6834-7-70>.
- [7] G. Breuer, P.P. Lamers, D.E. Martens, R.B. Draisma, R.H. Wijffels, Effect of light intensity, pH, and temperature on triacylglycerol (TAG) accumulation induced by nitrogen starvation in *Scenedesmus obliquus*, *Bioresour. Technol.* 143 (2013) 1–9, <http://dx.doi.org/10.1016/j.biotech.2013.05.105>.
- [8] I.T.D. Cabanelas, M. van der Zwart, D.M.M. Kleinegris, M.J. Barbosa, R.H. Wijffels, Rapid method to screen and sort lipid accumulating microalgae, *Bioresour. Technol.* (2014), <http://dx.doi.org/10.1016/j.biotech.2014.10.057>.
- [9] Y. Chisti, Biodiesel from microalgae beats bioethanol, *Trends Biotechnol.* 26 (2008) 126–131, <http://dx.doi.org/10.1016/j.tibtech.2007.12.002>.
- [10] Y. Chisti, J. Yan, Energy from algae: current status and future trends, *Appl. Energy* 88 (2011) 3277–3279, <http://dx.doi.org/10.1016/j.apenergy.2011.04.038>.
- [11] M.S. Cooper, W.R. Hardin, T.W. Petersen, R.A. Cattolico, Visualizing “green oil” in live algal cells, *J. Biosci. Bioeng.* 109 (2010) 198–201, <http://dx.doi.org/10.1016/j.jbiosc.2009.08.004>.
- [12] T.T.Y. Doan, J.P. Obbard, Enhanced intracellular lipid in *Nannochloropsis* sp. via random mutagenesis and flow cytometric cell sorting, *Algal Res.* 1 (2012) 17–21, <http://dx.doi.org/10.1016/j.algal.2012.03.001>.
- [13] R. Erickson, R. Jimenez, Microfluidic cytometer for high-throughput measurement of photosynthetic characteristics and lipid accumulation in individual algal cells, *Lab Chip* 13 (2013) 2893–2901, <http://dx.doi.org/10.1039/c3lc41429a>.
- [14] T. Govender, L. Ramanna, I. Rawat, F. Bux, BODIPY staining, an alternative to the Nile Red fluorescence method for the evaluation of intracellular lipids in microalgae, *Bioresour. Technol.* 114 (2012) 507–511, <http://dx.doi.org/10.1016/j.biotech.2012.03.024>.
- [15] M.J. Griffiths, C. Garcin, R.P. van Hille, S.T.L. Harrison, Interference by pigment in the estimation of microalgal biomass concentration by optical density, *J. Microbiol. Methods* 85 (2011) 119–123, <http://dx.doi.org/10.1016/j.mimet.2011.02.005>.
- [16] M.J. Griffiths, S.T.L. Harrison, Lipid productivity as a key characteristic for choosing algal species for biodiesel production, *J. Appl. Phycol.* 21 (2009) 493–507, <http://dx.doi.org/10.1007/s10811-008-9392-7>.
- [17] S.H. Ho, C.Y. Chen, J.S. Chang, Effect of light intensity and nitrogen starvation on CO₂ fixation and lipid/carbohydrate production of an indigenous microalga *Scenedesmus obliquus* CNW-N, *Bioresour. Technol.* 113 (2012) 244–252, <http://dx.doi.org/10.1016/j.biotech.2011.11.133>.
- [18] John A. Berges, David C. Mauzerall, Paul G. Falkowski, D.O.C., Differential effects of nitrogen limitation on photosynthetic efficiency of photosystems I and II in microalgae, *Plant Physiol.* 110 (1996) 689–696.
- [19] A.J. Klok, D.E. Martens, R.H. Wijffels, P.P. Lamers, Simultaneous growth and neutral lipid accumulation in microalgae, *Bioresour. Technol.* 134 (2013) 233–243, <http://dx.doi.org/10.1016/j.biotech.2013.02.006>.
- [20] A.J. Klok, J.A. Verbaanderd, P.P. Lamers, D.E. Martens, A. Rinzema, R.H. Wijffels, A model for customising biomass composition in continuous microalgae production, *Bioresour. Technol.* 146 (2013) 89–100, <http://dx.doi.org/10.1016/j.biotech.2013.07.039>.
- [21] H.J. La, J.Y. Lee, S.G. Kim, G.G. Choi, C.Y. Ahn, H.M. Oh, Effective screening of *Scenedesmus* sp. from environmental microalgae communities using optimal sonication conditions predicted by statistical parameters of fluorescence-activated cell sorting, *Bioresour. Technol.* 114 (2012) 478–483, <http://dx.doi.org/10.1016/j.biotech.2012.02.140>.
- [22] D.A. Ladner, D.R. Vardon, M.M. Clark, Effects of shear on microfiltration and ultrafiltration fouling by marine bloom-forming algae, *J. Membr. Sci.* 356 (2010) 33–43, <http://dx.doi.org/10.1016/j.memsci.2010.03.024>.
- [23] Liam Brennan, Anika S. Mostaert, Philip Owende, A.B.F., Enhancement of BODIPY 505/515 lipid fluorescence method for applications in biofuel-directed microalgae production, *J. Microbiol. Methods* 90 (2012) 137–143.
- [24] M. Chihara, I. Inoue, M. Kodama, T.N. *Chlorococcus littorale*, a new marine green coccoid alga (*Chlorococcales, Chlorophyceae*), *Arch. Protistenkd.* 144 (1994) 227–235.
- [25] T.M. Mata, A.A. Martins, N.S. Caetano, Microalgae for biodiesel production and other applications: a review, *Renew. Sust. Energ. Rev.* 14 (2010) 217–232, <http://dx.doi.org/10.1016/j.rser.2009.07.020>.
- [26] K. Matsumura, T. Yagi, A. Hattori, M. Soloviev, K. Yasuda, Using single cell cultivation system for on-chip monitoring of the interdivision timer in *Chlamydomonas reinhardtii* cell cycle, *J. Nanobiotechnol.* 8 (2010) 23, <http://dx.doi.org/10.1186/1477-3155-8-23>.
- [27] N.H. Norsker, M.J. Barbosa, M.H. Vermue, R.H. Wijffels, Microalgal production—a close look at the economics, *Biotechnol. Adv.* 29 (2011) 24–27, <http://dx.doi.org/10.1016/j.biotechadv.2010.08.005>.
- [28] M. Ota, Y. Kato, H. Watanabe, M. Watanabe, Y. Sato, R.L. Smith Jr., H. Inomata, Fatty acid production from a highly CO₂ tolerant alga, *Chlorococcus littorale*, in the presence of inorganic carbon and nitrate, *Bioresour. Technol.* 100 (2009) 5237–5242, <http://dx.doi.org/10.1016/j.biotech.2009.05.048>.
- [29] R. Praveenkumar, K. Shameera, G. Mahalakshmi, M.A. Akbarsha, N. Thajuddin, Influence of nutrient deprivations on lipid accumulation in a dominant indigenous microalga *Chlorella* sp., BUM11008: evaluation for biodiesel production, *Biomass Bioenergy* 37 (2012) 60–66, <http://dx.doi.org/10.1016/j.biombioe.2011.12.035>.
- [30] M. Terashima, E.S. Freeman, R.E. Jinkerson, M.C. Jonikas, A fluorescence-activated cell sorting-based strategy for rapid isolation of high-lipid *Chlamydomonas* mutants, *Plant J.* 81 (2015) 147–159, <http://dx.doi.org/10.1111/tpj.12682>.
- [31] J.G. Umen, U.W. Goodenough, Control of cell division by a retinoblastoma protein homolog in *Chlamydomonas*, *Genes Dev.* 15 (2001) 1652–1661, <http://dx.doi.org/10.1101/gad.89210>.
- [32] G. Van Vooren, F. Le Grand, J. Legrand, S. Cuiné, G. Peltier, J. Pruvost, Investigation of fatty acids accumulation in *Nannochloropsis oculata* for biodiesel application, *Bioresour. Technol.* 124 (2012) 421–432, <http://dx.doi.org/10.1016/j.biotech.2012.08.009>.
- [33] N. Velmurugan, M. Sung, S. Yim, M.S. Park, J. Yang, K. Jeong, Systematically programmed adaptive evolution reveals potential role of carbon and nitrogen pathways during lipid accumulation in *Chlamydomonas reinhardtii*, *Biotechnol. Biofuels* 7 (2014) 117, <http://dx.doi.org/10.1186/s13068-014-0117-7>.
- [34] R.H. Wijffels, M.J. Barbosa, An outlook on microalgal biofuels, *Science* 329 (2010) 796–799, <http://dx.doi.org/10.1126/science.1189003>.
- [35] T.-T. Yen Doan, J.P. Obbard, Enhanced lipid production in *Nannochloropsis* sp. using fluorescence-activated cell sorting, *GCB Bioenergy* 3 (2011) 264–270, <http://dx.doi.org/10.1111/j.1757-1707.2010.01076.x>.
- [36] Yueli Jiang, Antonietta Quigg, T.Y., Photosynthetic performance, lipid production and biomass composition in response to nitrogen limitation in marine microalgae, *Plant Physiol. Biochem.* 54 (2012) 70–77.